

DEVELOPMENT OF MICROMORPH CELLS IN LARGE-AREA INDUSTRIAL REACTOR

N. Wyrsh, A. Billet, G. Bugnon, M. Despeisse, A. Feltrin, F. Meillaud, G. Parascandolo, C. Ballif
Ecole Polytechnique Fédérale de Lausanne (EPFL), Institute of Microengineering (IMT), Photovoltaics and thin-film electronics laboratory, Breguet 2, CH-2000 Neuchâtel, Switzerland

ABSTRACT: The influences of the deposition pressure and silane depletion on the efficiency of single-junction microcrystalline silicon solar cells has been investigated. The efficiency is found to correlate with the ion energy which affects the density of states in the absorber material. Cell with efficiency of 7.3% at a deposition rate of 1 nm/s, and, respectively, 7.8% at 0.35 nm/s were deposited in R&D KAI M industrial reactor. Silicon oxide based intermediate reflector layers were developed in KAI reactor for incorporation in micromorph devices. Material with an index of refraction of 1.7 at 600 nm and low lateral conductivity were deposited. Micromorph devices incorporating these intermediate reflector layers were fabricated with initial efficiency of 12.3% at a deposition rate of 0.35 nm/s and 10.8% at 1 nm/s.

Keywords: a-Si:H, micro crystalline silicon, tandem, light trapping

1 INTRODUCTION

Successful industrial development of micromorph modules are critically dependant on their cost to performance ratio. The improvement of the latter calls for an increase in the cell efficiency while reducing the deposition time by increasing the deposition rate. Progressing towards these objectives, micromorph tandem devices with initial efficiency of up to 13.3% have been recently obtained in small area reactor at IMT Neuchâtel [1]. Such high efficiencies were achieved thanks to the development of an in-situ silicon oxide based intermediate reflector (SOIR) layer [2]. Intermediate reflectors are used to increase the current density in thin top amorphous cells of micromorph tandem devices [3]. For that purpose a material with a low refractive index is necessary. The challenge in the optimization of these layers is to lower the refractive index without compromising the electrically conductive properties. These developments of the micromorph cells (including SOIR) in small area system operating at 70 MHz were transferred to an industrial R&D KAI S and KAI M systems operated at 40.68 MHz.

Deposition rate is a key issue for industrial application. In order to achieve high deposition rate with the least detrimental effects on the material quality, several regimes of deposition pressure and silane depletion have been studied for the deposition of single junction microcrystalline silicon ($\mu\text{c-Si:H}$) cells. Two regimes leading to a deposition rate of 0.35 nm/s and of 1 nm/s were selected for the development of micromorph tandem devices incorporating also SOIR layers. The effect of the inter-electrode on the efficiency of single-junction $\mu\text{c-Si:H}$ cells was also investigated in the case of the high deposition rate regime.

2 EXPERIMENTAL

Single-junction and tandem micromorph solar cells were deposited in p-i-n configuration on AF45 glass substrate covered with ZnO:B deposited by LP-CVD (low pressure chemical vapor deposition) in industrial R&D PE-CVD (plasmas enhanced CVD) KAI S or KAI M reactor operated at 40.68 MHz. Similar ZnO:B layers were also used as back contact for all cells. A surface treatment of the ZnO front contact was applied and a dielectric white reflector was added to the back contact.

More details on the deposition conditions can be found in [4].

Degradation of the cells has been performed at 50°C under a white light illumination (at approx. 100 mW/cm²) from a metal halide HQI lamp and in open circuit condition.

SOIR layers were prepared from a mixture of SiH₄, CO₂, H₂ and PH₃ gases in our large-area (37x47 cm²) very-high frequency (VHF) PECVD KAI-S system at 40.68 MHz. The development of SOIR layers was done on layers of roughly 100 nm deposited directly on glass to assess the conductivity, the crystalline fraction through Raman scattering experiment and the refractive index value. The latter was found from fitting the ellipsometry measurements to a Tauc-Lorentz dispersion model including a surface roughness layer. The thickness was measured with a height profiler. Infrared (IR) absorption measurements were performed with a Nicolet 8700 system from Thermo on samples deposited on intrinsic, one-side polished wafers. The absorption spectra were normalized with the layer thickness.

3 RESULTS AND DISCUSSION

3.1 SiO_x intermediate reflector (SOIR)

The influence of multiple parameters was studied in regard to the quality of the material, among which: deposition pressure, power density, total gas flow,

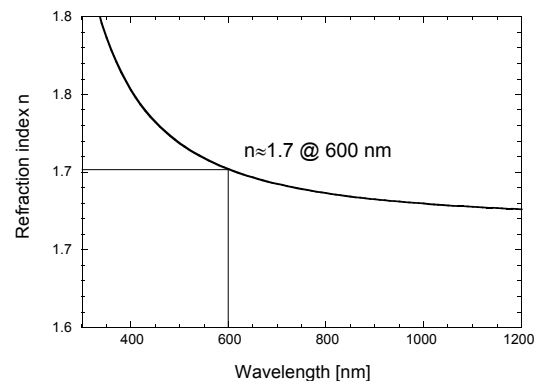


Figure 1: Refractive index n as a function of wavelength with $n \approx 1.7$ at 600nm of a nc-SiO_x layer obtained in the KAI-S system.

hydrogen dilution, and CO₂ fraction. As already observed in material deposited in small area systems [2], these layers are made of n-doped mixed-phase material which consists of silicon nano-crystallites incorporated into an amorphous SiO_x matrix (nc-SiO_x). These nano-crystallites most likely insure current flow through the layer. The main requirements for the use of this mixed-phase material when used in a micromorph cell, is to have the lowest refraction index while providing a sufficiently high transverse conductivity σ (we typically target a value below $10^{-6} \Omega^{-1} \text{cm}^{-1}$ for our micromorph devices). To evaluate the relevant deposition parameters on which these two values n and σ ultimately depend, numerous deposition series were conducted. The index of refraction as a function of wavelength for the “best” layers is plotted in Fig. 1. This close to the optimum material (for our micromorph device) exhibits an index of refraction $n \approx 1.7$ (at 600 nm) with a lateral conductivity of $\approx 10^{-7} \Omega^{-1} \text{cm}^{-1}$.

3.2 Microcrystalline silicon single-junction cells

A reduced ion bombardment is assumed to be necessary for getting device quality $\mu\text{-Si:H}$ layers and for achieving high efficiency in $\mu\text{-Si:H}$ solar cells. As one can observe in Fig. 2, higher efficiency is obtained when the deposition pressure is increased. Higher silane depletion conditions favor low ion bombardment too, leading to a marked improvement, especially at low pressure, as also demonstrated by the results of Fig. 2. The ion energy values were here deduced from the measurement of the V_{pp} using a simple model for the ion bombardment presented in Ref. [4]. Silane depletion greatly affects solar cell efficiencies at lower pressures, whereas at higher pressure values its impact is diminished. The reduction in the cell efficiency is correlated with an increase in the defect density as observed by FTPS measurements of $\mu\text{-Si:H}$ intrinsic layers included in these solar cells: with increasing pressure and silane depletion the defect density is significantly lowered as presented in [4]. However chemical aspects, such as gas phase reactions and type of silane radicals are likely to play a role as well.

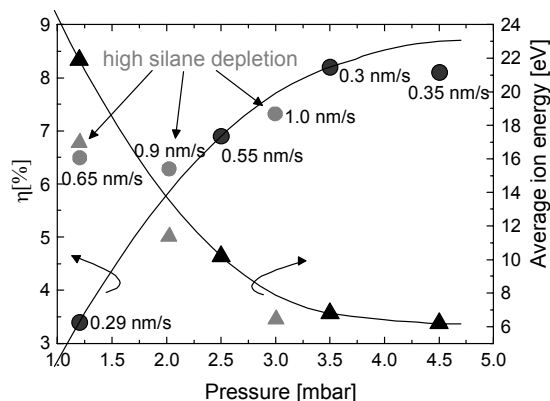


Figure 2: Solar cell efficiencies as a function of the deposition pressure (circles). The mean ion energy was calculated for each deposition regime (triangles). High silane depletion regimes are indicated in grey. The lines are a guide to the eye

As seen in Fig. 2, best solar cells are deposited at 0.35 nm/s, at high pressure, under high silane depletion. The best cell with an efficiency of 8.2% was obtained at

a deposition rate of 0.3 nm/s with efficiency. The effect of cell thickness for the latter growth regime is illustrated in Fig. 3 for two values of the cell thickness. Increasing the thickness from 1 to 2.7 μm leads to a significant reduction of both the open circuit voltage and the fill-factor. As one can observe in Fig. 4, a large thickness improves the red and infra red light response of the cell but results in a loss of the blue response due to an insufficient optimization of the p or p-i interface.

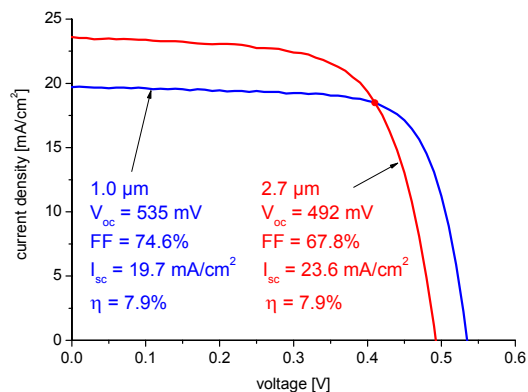


Figure 3: I(V) characteristics of 2 $\mu\text{-Si:H}$ single-junction cells (of 1 and 2.7 μm) deposited at 0.35 nm/s.

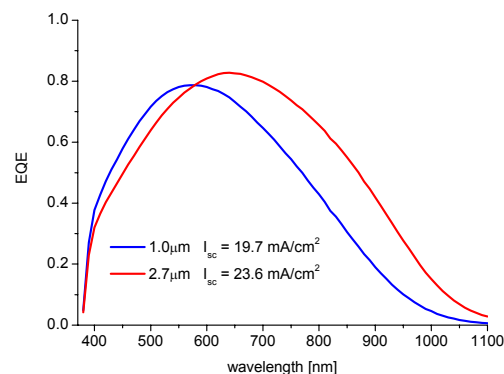


Figure 4: External quantum efficiency EQE of the 2 $\mu\text{-Si:H}$ single-junction cells as plotted in Fig. 3.

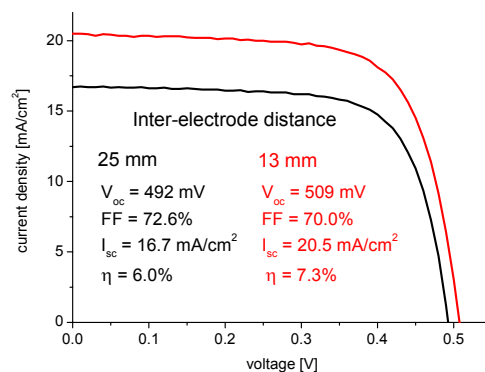


Figure 5: I(V) characteristics of 2 $\mu\text{-Si:H}$ single-junction cells deposited under similar deposition conditions at 1 nm/s with two different inter-electrode distance (13 and 25 mm).

High rate deposition (1 nm/s) of $\mu\text{-Si:H}$ at plasma excitation frequencies above 13.56 MHz requires a reduction of the inter-electrode distance to achieve high performance. As observed in Fig. 5 a decrease of the inter-electrode distance from 25 to 13 mm allows for a

marked improvement of the cell performance. The reduction of powder formation, combined with higher working pressures at 13 mm inter-electrode gap are probably the reason for can the better efficiency.

3.3 Micromorph tandem cells

A $\mu\text{-Si:H}$ cell deposited at 1 nm (as presented in section 3.2) was incorporated into tandem device. The respective component cell thicknesses are 220 nm for the top and 1.8 μm for the bottom one. The I(V) characteristics as well as the external quantum efficiency EQE are presented in Fig. 6. Light-soaking of the tandem reduces the efficiency by 11% resulting in a stable value of 9.6%. As seen in Fig. 6, most of the degradation can be attributed to the top cell even while a reduction of the infra-red response is due to the a smaller $\mu\text{-Si:H}$ bottom cell degradation. The relatively low overall degradation is here obtained thanks to the thin top cell. One can also observe that the cells are rather well “current matched” for both the annealed as the degraded state.

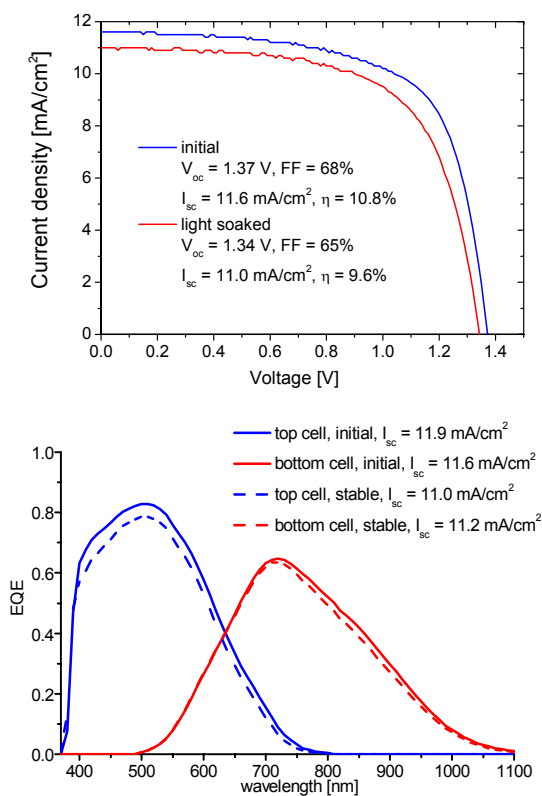


Figure 6: I(V) characteristics and external quantum efficiency of our best micromorph device (thickness of 220 nm and 1.8 μm , 1.2 cm^2) with a microcrystalline bottom cell deposited at 1 nm/s.

$\mu\text{-Si:H}$ cells deposited at a lower deposition rate of 0.35 nm were also incorporated in a tandem devices. Best initial efficiency of 12.3% (see Fig. 7) was obtained so far with component cell thickness of 250 nm and 2.7 μm , and the implementation of a SOIR layer and a broad band anti-reflective layer. The lower open circuit voltage, compared to the previous micromorph cell is here due to the use of a rougher front ZnO contact. As deduced from the EQE data, a remarkable total current of 26.2 mA/cm² was obtained for this tandem device. Stability test of this cell is in progress and the degradation is expected to be approximately 15%.

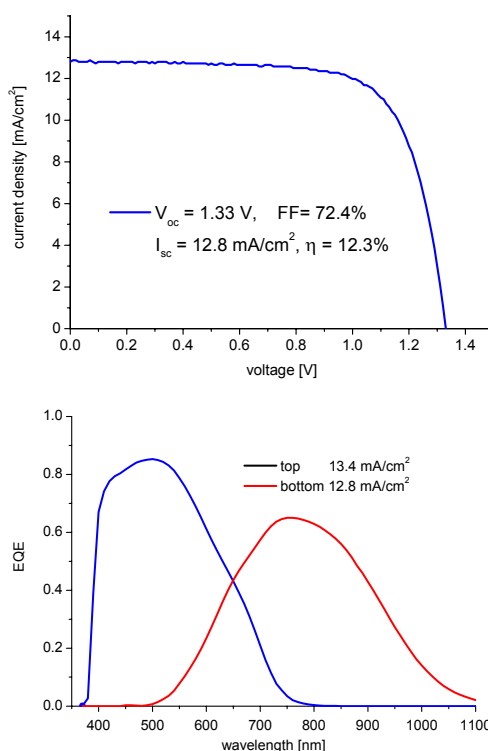


Figure 7: I(V) characteristics and external quantum efficiency of our best micromorph device (thickness of 250 nm and 2.7 μm , 1.2 cm^2) with a microcrystalline bottom cell deposited at 0.35 nm/s. A SOIR and a broad-band anti-reflection coating on the glass substrate were also implemented.

4 CONCLUSIONS

The efficiency of $\mu\text{-Si:H}$ single junction cell is found to correlate with the energy of the ions impinging on the growing surface. Lower ion energy ions reduces the material defect density. Consequently, the efficiency increases with increasing power and silane depletion.

For optimized devices the initial efficiency is decreased from 8.2% to 7.3% as the deposition rate increases from 0.3 nm/s to 1.0 nm/s. Incorporating such cell in a micromorph device (with an SiO_x intermediate reflector), an initial efficiency of 10.8% and stable efficiency of 9.6% have been so far obtained with a microcrystalline cell of 1.8 μm deposited at 1 nm/s in an industrial R&D KAI M reactor.

At a lower deposition rate of 0.35 nm/s (also in a KAI M reactor), initial efficiency of 12.3% with a total current of 26.2 mA/cm² have been obtained for a micromorph tandem with an SiO_x intermediate reflector and a 2.7 μm bottom cell.

Further improvement is expected from a better current matching of the device and further optimization of the $\mu\text{-Si:H}$ cell growth.

5. ACKNOWLEDGMENTS

This work was financially supported by the Swiss National Office for Energy and by the EU integrated project Athlet.

6 REFERENCES

- [1] D. Dominé et al., Proc. of the 23rd EU-PVSEC (2008)
- [2] P. Buchlmann et al, APL. 91 (2007) 143505.
- [3] D. Dominé et al., Phys. stat. sol. (RRL) 2 (2008) 163.
- [4] G. Bugnon et al, JAP 105 (2009) 064507